



HAL
open science

Nanocarb-21: a miniature Fourier-Transform spectro-imaging concept for a daily monitoring of greenhouse gas concentration on the earth surface

S. Gousset, E. Le Coarer, N. Guerineau, L. Croizé, T. Laveille, Y. Ferrec

► **To cite this version:**

S. Gousset, E. Le Coarer, N. Guerineau, L. Croizé, T. Laveille, et al.. Nanocarb-21: a miniature Fourier-Transform spectro-imaging concept for a daily monitoring of greenhouse gas concentration on the earth surface. ICSO 2016, Oct 2016, BIARRITZ, France. hal-01401371

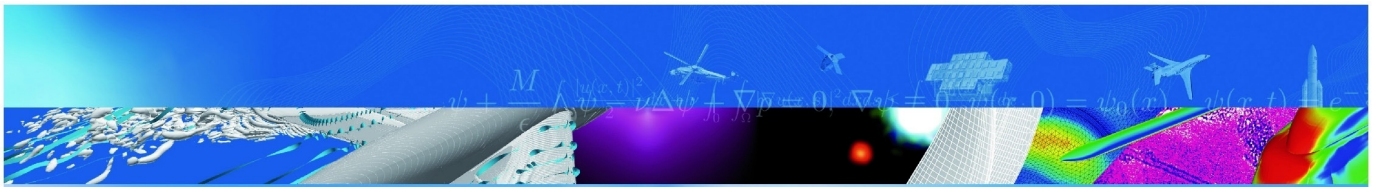
HAL Id: hal-01401371

<https://hal.science/hal-01401371>

Submitted on 23 Nov 2016

HAL is a multi-disciplinary open access archive for the deposit and dissemination of scientific research documents, whether they are published or not. The documents may come from teaching and research institutions in France or abroad, or from public or private research centers.

L'archive ouverte pluridisciplinaire **HAL**, est destinée au dépôt et à la diffusion de documents scientifiques de niveau recherche, publiés ou non, émanant des établissements d'enseignement et de recherche français ou étrangers, des laboratoires publics ou privés.



COMMUNICATION A CONGRES

**Nanocarb-21: a miniature
Fourier-Transform spectro-imaging
concept for a daily monitoring of
greenhouse gas concentration on
the earth surface**

S. Gousset (IPAG), E. Le Coarer (IPAG),
N. Guerineau, L. Croize, T. Laveille, Y. Ferrec

ICSO 2016
BIARRITZ, FRANCE
18-21 octobre 2016

TP 2016-671

70 2016
ans

ONERA

THE FRENCH AEROSPACE LAB

NANOCARB-21: A MINIATURE FOURIER-TRANSFORM SPECTRO-IMAGING CONCEPT FOR A DAILY MONITORING OF GREENHOUSE GAS CONCENTRATION ON THE EARTH SURFACE

S. Gousset¹, E. Le Coarer^{1,3}, N. Guérineau², L. Croizé², T. Laveille², Y. Ferrec²

¹Univ. Grenoble Alpes, CNRS, IPAG, F-38000 Grenoble, France. ²ONERA, France. ³CSUG, France.
silvere.gousset@univ-grenoble-alpes.fr

I. INTRODUCTION

Earth's positive radiative forcing is significantly accelerated by massive anthropogenic emissions of greenhouse gases, like carbon dioxide and methane [1]. Since 2014 the concentration of CO₂ exceeds 400 parts per million (ppm), and the concentration of CH₄ climbs up to 1900 parts per billion (ppb) [2] with a constant annual increase. Thereby it is a major issue to quantify the impact and potential disturbances induced on the geophysical natural carbon cycle. To better constrain climate models, it is important to improve our knowledge of CO₂ fluxes between terrestrial reservoirs (biosphere, atmosphere and ocean) and to be able to distinguish natural and anthropogenic sources and sinks of carbon. Currently, a few space missions are dedicated to the monitoring of greenhouse gas concentration, such as OCO and GOSAT, potentially soon relayed by ESA mission CarbonSat and CNES mission MicroCarb. This spatial constellation is backed on ground by a network of stations. The ultimate goal is to be able to monitoring the greenhouse gas emission from local (city) to global scale (Earth) systematically at any time [3]. Nevertheless, the revisit frequency is not yet sufficient to reach a daily coverage. There is also not real continuous sampling of the surface (only obtain by averaging data over time).

Within this context we propose the NanoCarb-21 space mission, to complete the observational data flows with high spatially resolved daily data, additionally to the MicroCarb mission. This goal requires a large constellation of satellites in orbit at a given moment. We can realistically achieve this by considering nanosatellites, cheaper to develop, product and launch. It is a huge challenge to make science with a cubesat, considering miniaturization issues of the payload. Thus we cannot aim to be independent of MicroCarb mission and of the existing constellation, for example concerning the limited on-board calibration systems.

We present in this paper the design of an ultra-compact imaging spectrometer for the NanoCarb-21 mission, based on the last developments about μ SPOC (Spectrometer on Chip) technology at the ONERA and IPAG. We firstly describe the preliminary mission elements in the section II. Then the section III presents the payload, by detailing μ SPOC technology, conversion into imaging-spectrometer, and the current optical/implementation design. We finally expose in the sections IV and V our pre-phase-0 studies, consisting in optimizing the design, maximizing the sensitivity, and predicting some performances, according to numerical simulations presented in the section IV.

II. FIRST MISSION ELEMENTS

The NanoCarb mission has been designed complementary to the CNES MicroCarb mission, in order to complete the current global greenhouse gas survey network by a specific data production. At data product level 1 (e.g. calibrated spectra), the missions will provide to temporally and spatially increase the data flow about CO₂ and CH₄ absorption in the atmosphere, and also about geophysical biases, such as scattering effects due to aerosols, water vapor and clouds. At level 2, we expect to enhance spatial coverage and temporal resolution of the specie concentration maps retrieved by model inversion. Therefor the mission elements will be based on the other greenhouse dedicated missions such as MicroCarb. We have considered a LEO sun-synchronous orbit, probably at an altitude of 594 km, and a constant local time of 11:30. Due to precession, this kind of orbit allows to cover the Earth's surface with a monthly delay (10-25 days). By placing each of the 21 nanosatellites in this orbit with an interval of approximately 5 minutes, the NanoCarb mission provides a daily coverage of the Earth. The Earth's surface will be sampled continuously by a spectro-imager embedded in each unit of the constellation, providing a high spatial resolution of 9 km² for a 150 km-wide swath, which is consistent with emission or sink phenomena at local scale. The science instrument is also based on actual/scheduled missions, by observing the solar light reflected on the Earth's surface and scattered by the atmosphere. We expect to implement two modes: nadir observations above emerged land and glint mode above the oceans (low albedo) in order to increase collected light. The required sensibility is better than 3 ppm of CO₂ with a goal at 1 ppm, and 12 ppb of CH₄. In the same way of MicroCarb, CarbonSat or GOSAT, three main spectral bands are currently considered: 1.6 μ m, 2.06 μ m and 760 nm. The 1.6 and 2.06 μ m bands present some absorption lines due to atmospheric CO₂ and CH₄. The 760 nm band is dedicated to the measure of atmospheric pressure (O₂ concentration), scattering (aerosols) and water

vapor effects. The main issue of the NanoCarb mission is to design a compact imaging spectrometer. We describe such a payload in the next section.

III. A MICROSPOC-BASED IMAGING FOURIER TRANSFORM SPECTROMETER

A. μ SPOC principle and assets

We designed the NanoCarb payload to take advantage of the latest joint developments between ONERA and IPAG about compact spectrometry. Therefore it will be based on the integrated Fourier Transform Spectrometer (FTS) family so-called SPOC (SPectrometer On Chip) [4]. This concept consists in introducing a continuous modulation of the Optical Path Difference (OPD - δ) in the chip in one direction, forming 2-waves interferometric fringes directly on the photo-sensitive surface. In the simple way the OPD modulation is introduced by an interferometric element, such as a glass slide or a prism glue to the sensor. The Fig. 1 shows such a spectrometer, and we can see to the right an example of 2D-interferogram obtained with a monochromatic and uniform illumination (912nm strong line of Argon). A Fourier transform provides to obtain the incident light spectrum. By opposite to the SIFTI FTS [5], a μ SPOC is a fully passive bulk spectrometer without mobile components. Hence it is potentially less sensitive to thermal and mechanical biases. It is also very simple to thermalize it with a drastic reduced power consumption due to its extreme compactness, which is promising for on-board spectrometry. The design Fig. 1 has been adapted in this way for the incoming ATISE nanosat mission of the Grenoble Spatial Center University (CSUG) to detect auroral emission lines in the upper atmosphere [6]. Parallel developments affecting the NanoCarb mission consist of an adaptation of the concept to the spectro-imagery, with drastic miniaturization issues.

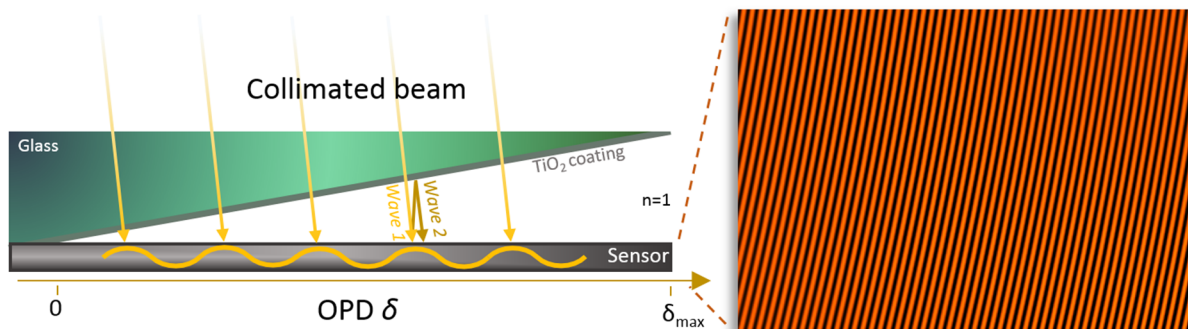


Fig. 1. SPOC principle. Left: OPD modulation between glass prism and chip, responsible for 2-waves interferences on the sensor surface; Right: 2D-interferogram obtained with the strong line of Argon at 912 nm and a uniform illumination.

B. Conversion into micro-imaging spectrometer for NanoCarb

We describe in the following paragraphs the SPOC imaging spectrometer of NanoCarb, giving its principle and the relevant design issues. Then we detail its implementation in a cubesat. To introduce some imagery feature we proceed to a discretization of the initially continuous OPD modulation. Thus the sensor is now divided into thumbnails or sub-apertures, each one coding for only one OPD of the interferogram. The field is imaged over the thumbnails and modulated according to the OPD. To retrieve the interferogram contrast at a given OPD for one point of the imaged field, we take advantage of the satellite scrolling over the time, inducing a pixel displacement on the thumbnail and so an intensity modulation according to the introduced OPD. A pixel line of the thumbnail corresponds to the ground satellite swath.

In the most up-to-date design, we expect to implement a 1024x1024 NGP sensor from SOFRADIR [7], sensitive from 400 nm to 3-4 μ m with a Read Out Noise (RON) about 150 electrons. The photo-sensitive chip area will be divided into four 500x500 pixels independent sub-areas. Each one will be dedicated to the specific spectral bands described in the previous section, then divided into 100 50x50 pixels thumbnails (e.g. 100 OPD) as shown Fig. 2-right. The channel number 3 is not yet currently allocated and allows to adapt potentially the instrument to another spectral band for complementary measures as required (bias mitigation for example). One pixel represents a 3x3 km resolution element of the imaged field.

C. Optical implementation

The Fig. 2-left shows the current optical design of the four-band imaging spectrometer. A very small 3 mm-diameter telescope is required in order to respect the Jaquinot criterion about aperture [4] and the field constraints.

The device (including the chip) is easily contained in a $150 \times 40 \times 40 \text{ mm}^3$ very compact area, which is also simple to be thermally regulated at 200 K.

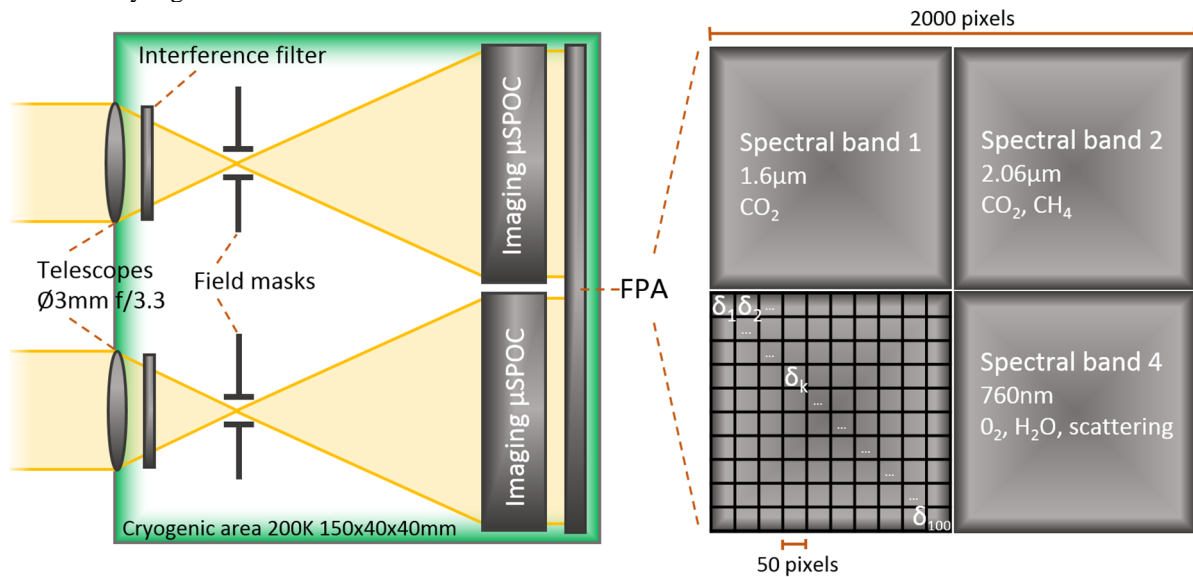


Fig. 2. Left: optical design of the four band imaging spectrometer SPOC; Right: spectral band allocation over the chip. Each spectral band is divided into 100 square sub-apertures coding for 100 different OPD δ_k .

Such a compact instrument is fully compatible with a 6U cubesat ($30 \times 20 \times 10 \text{ cm}^3$) as shown Fig. 3. About 2U are allocated to the optical bloc including the chip and the cooling device. The remaining space could be dedicated to the control electronic boards, communication and navigation systems, with most of the components available off-the-shelf. The estimated mass of the payload is about 6-7 kg, for a total power consumption of 10 W including cooling. We estimate a data flow about 21 Go/day with compression, and 3.6 Go/day with on-board data processing.

The main issue of the instrument design is now to identify some interest fringes on the interferogram, that will be sampled at the OPD δ_k . Thus we have to optimize the instrumental sensitivity to a given variation of the CO_2 or CH_4 concentration. We have also to identify in the interferogram some geophysical bias (aerosols) signatures. This study is based on numerical simulations, presented in the next section.

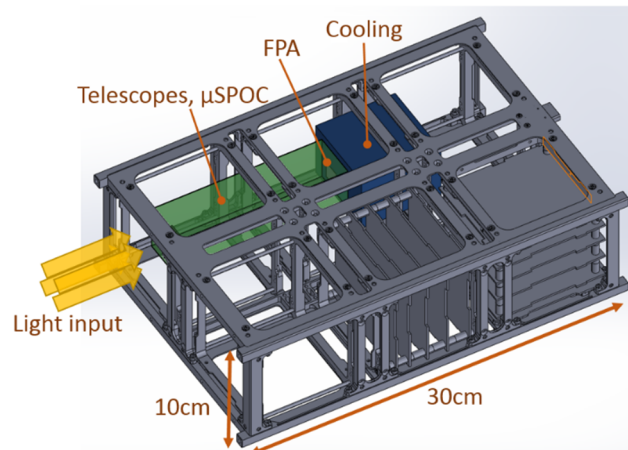


Fig. 3. Imaging micro-SPOC implementation example in a 6U cubesat platform from ISIS.

IV. NUMERICAL SIMULATIONS

We simulated atmospheric absorption spectra at the ONERA using MODTRAN (Release 5.2.1) [8] radiative transfer code, in several typical observation scenarios. We use these synthetic spectra at IPAG to compute theoretical interferograms and derive sensibility and design assessments. In the following paragraphs we firstly give the simulation parameters, then the observational scenario. We finally present the theoretical interferogram in the interest spectral bands in order to discuss about measurement strategy for concentration retrieval.

MODTRAN 5 reaches a spectral resolution of 0.1 cm^{-1} which is consistent with atmospheric absorption line width. In this paper we focus only on the measurement of CO_2 concentration in the averaged column density. We

have not yet consistent simulated data with different profiles of concentrations of CH₄. The atmosphere composition model is the US standard. We simulated spectra with CO₂ concentration from 400 to 430 ppm. The nominal concentration is taken at 400 ppm, near to the actual annual and global averaged value. Different kind of aerosol models have been tested as reported in Tab. 1. We have reported also the averaged luminance in the spectral bands 1 and 2, obtained with a surface albedo of 0.3, and a solar zenithal angle of 20°. We compared these values to a CNES scenario and we could report it as a medium flux condition, such as above emerged land at a tempered latitude with vegetation for example.

Tab. 1. Simulation parameters for MODTRAN radiative transfer code.

Range of CO₂ concentration	400-430 ppm	
Aerosol models	- NA - Rural, visibility: 23 km - Urban, visibility: 3 km - Desert	
Albedo	0.3	
Solar zenithal angle	20 °	
Temperature at ground	294 K	
Averaged luminance [W/m ² /sr/μm]	@1.6μm	19.38
	@2.06μm	4.69

We present on Fig. 4 the simulated 1.6 μm (left) and 2.06 μm (right) bands without aerosol, for a nominal CO₂ concentration of 400 ppm. The 1.6 μm band presents several regularly spaced unsaturated absorption lines, allowing to measure the CO₂ concentration. On the opposite the lines at 2.06 μm are saturated. Nevertheless, they can potentially bring some information about scattering effects as we will discuss in the next section.

Finally, we computed on Fig. 5 the corresponding theoretical interferogram for the full 1.6 μm band. Given the limited number of OPD per spectral band on the spectrometer, we can't sample all the interferogram and thus it is not possible to retrieve the full spectrum. Nevertheless, the FTS allows to recognize some specific motif in the spectrum. In our case we can observe Fig. 5 some bumps at 5.5 mm then 11 mm and 16.5 mm of OPD, corresponding in the dual space to the absorption line comb (period ~1.8 cm⁻¹). The fringe contrast in these region is directly proportional to the energy absorbed by CO₂, and thus to the CO₂ concentration (assuming small variations of concentration). Our samples will be placed between 5 and 6mm for the 1.6 μm band. In order to maximize the contrast in this region and the sensibility to the concentration of CO₂, we have to optimize the spectral window, that will be study in the next section. To conclude, we can also notice that a 1 ppm variation of column density CO₂ (goal) causes a luminance variation about 10⁻¹¹ W/cm²/sr/cm⁻¹ for a mean level about 10⁻⁷ W/cm²/sr/cm⁻¹ at 1.6 μm. We study also in the next section the capability of the instrument to measure such a small variation.

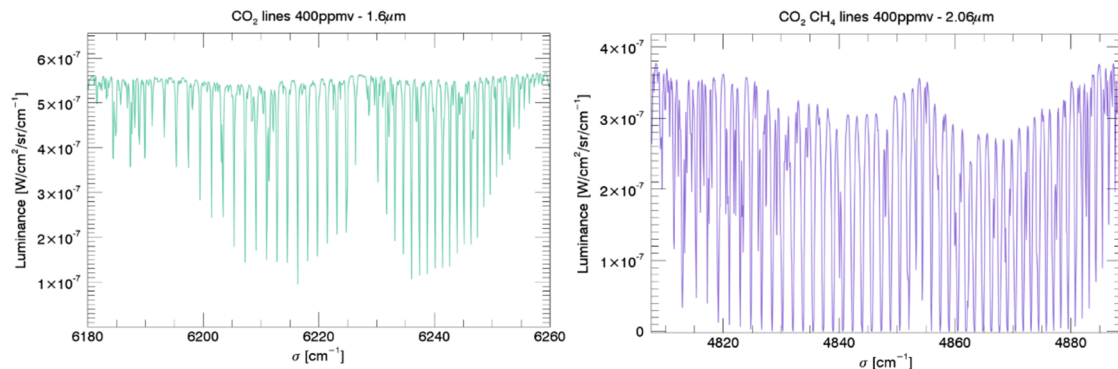


Fig. 4. MODTRAN simulations of absorption lines of atmospheric CO₂ at 1.6 μm (Left) and 2.06 μm (Right), for a concentration of 400 ppm.

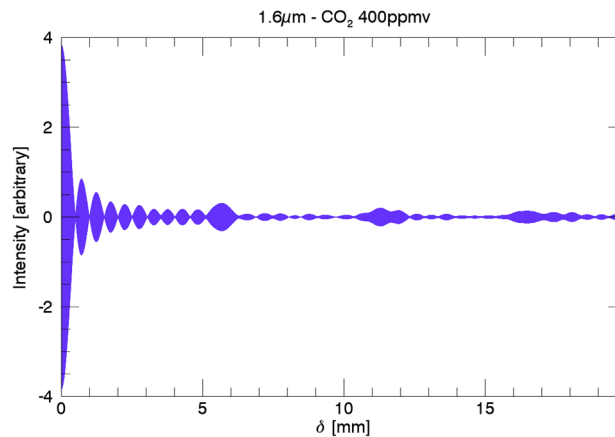


Fig. 5. Synthetic interferogram for the full band at $1.6\mu\text{m}$, a concentration of CO_2 of 400 ppm, and without taking account of aerosols. The bumps at 5.5, 11 and 16.5 mm are the signature in the direct space of the absorption line comb in the Fourier space.

V. SENSIBILITY STUDY

We present in this section a preliminary sensibility study based on the previous numerical simulations. First we optimize the NanoCarb design. Then we derive its effective performances with photometric considerations. To finish, we will quantify the bias causes by aerosols, and give some ways to mitigate it. For this study we consider partial differential interferograms, that we call Jacobian in the following of this paper. These are very useful tools to observe specific effects of tiny variations of the spectrum over the interferogram.

A. Sub-band optimization for CO_2 concentration measurement

The first work consists in optimizing the spectrometer sensibility to the concentration of CO_2 . To do that we fit a sub-band of the $1.6\mu\text{m}$ spectral band in order to maximize the contrast of the fringes between the 5 mm et 6 mm OPD according to the previous section. More the sub-band is large, more the collected flux is important, but potentially lesser the fringes are contrasted around 5.5 mm due to jitter in the line period. We scan the $1.6\mu\text{m}$ band with increasingly wide windows, and we compute for each the maximum value of the interferogram between 5 mm and 6 mm of OPD. The obtained figure of merit is shown Fig. 6. Each vertically-delimited area represents a given window width. The optimal value is found for a 30 cm^{-1} -wide window, centered around 6220 cm^{-1} . The corresponding Jacobian is shown Fig. 7 for a variation of the CO_2 concentration of 1 ppm. We can now place our 100 samples of OPD in the fringes around the maximum of the Jacobian (excluding the unity pic at 0 mm), where the sensibility to a variation of concentration is maximal.

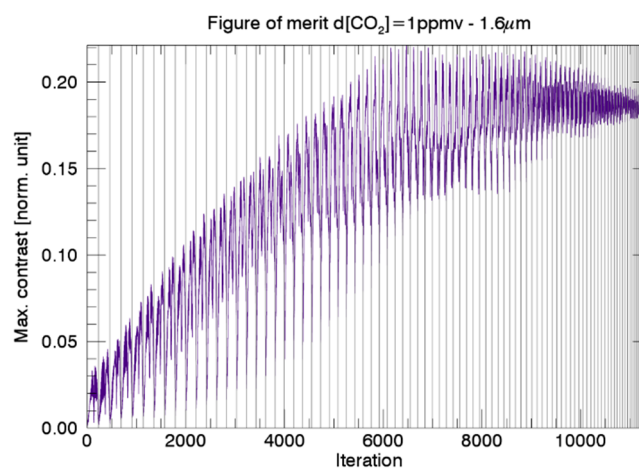


Fig. 6. Maximum of the Jacobian around 5.5 mm for a variation of 1 ppm of CO_2 according to the sub-band position and width in $1.6\mu\text{m}$ band.

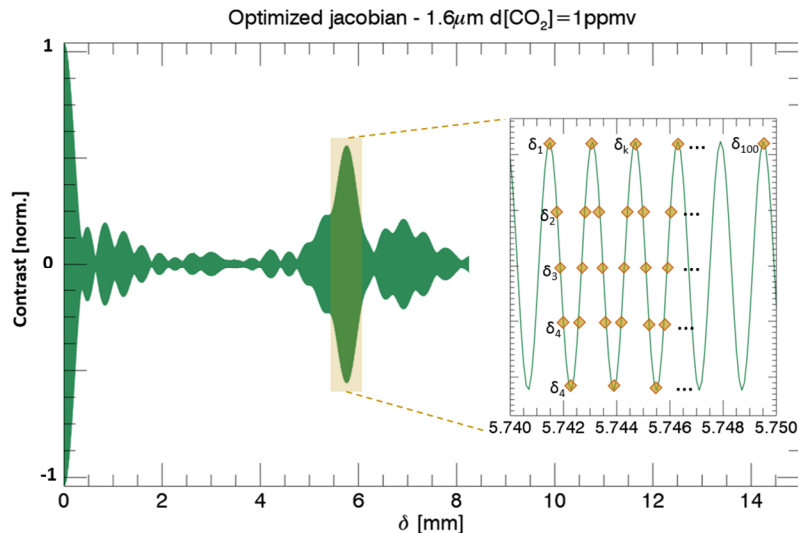


Fig. 7. Jacobian for a variation of 1 ppm of CO₂, and for the optimal sub-band of the 1.6 μm band. The fringes around the maximum of the Jacobian are sampled with the 100 OPD of the spectrometer.

B. Effective sensitivity, photometric elements

We can derive now from this study some photometric elements. To do that we introduce the Sensitivity-to-Noise Ratio (SNR_j), corresponding to the maximum of the Jacobian in electron compared to noise. For a Jacobian obtained with a variation of concentration of 1 ppm, a SNR_j greater than 1 indicates that the instrument can detect such a variation, given photometric data. SNR_j is given by:

$$SNR_j = \frac{n_{pix} n_{OPD} N_{jmax}}{\sqrt{n_{pix} n_{OPD} N_e + n_{pix} n_{OPD} \sigma_{RON}^2}} \quad (1)$$

With n_{pix} the number of pixel in the swath, n_{OPD} the number of sub-aperture per band, N_e the mean number of electron per frame and per pixel (derives from the spectral luminance), σ_{RON} the sensor RON and N_{jmax} the maximum illumination of the Jacobian. The SNR_j takes into account both photon and read out noises. We report on the Tab. 2 the results of this study. Given the SNR_j of 2.5 in our setup, we have demonstrated here the full capability of NanoCarb to detect a variation of the CO₂ concentration lesser than 1 ppm in medium flux conditions. We can notice also the convenient mean number of electron per frame and per pixel on the interferogram N_e for 1.6 μm band, despite of the very small telescope aperture (3 mm).

Tab. 2. Photometric elements for CO₂ concentration measurement.

Jacobian variation	d[CO ₂]=1 ppm
σ_{RON} [electron]	150
N_e [electron/frame/pixel]	134092
N_{jmax} [electron/frame/pixel]	14
SNR_j	2.5

C. Aerosol effects and mitigation

The previously computed intrinsic sensibility is not directly effective due to geophysical biases, affecting all the dedicated missions. The aerosols in the atmosphere are responsible for the main biases over the concentration estimation. Indeed, the induced scattering effects disrupt the optical path of light in the atmosphere, and introduced artificial variations of the measured concentration. They are mitigated only during the model inversion with priors extracted from *in situ* measurements. We propose in this paragraph an approach to extract information about aerosol from our data.

On the Fig. 8-top two Jacobians on the 1.6μm band are represented, the first one with a null differential of concentration, but with the introduction of rural-type aerosol. The second one without aerosol and a differential of the CO₂ concentration of 20 ppm. We notice that the aerosol induced a contrast variation at the same OPD than CO₂ absorption, and furthermore introduce a ~20 ppm-bias over the concentration measurement! Thus we can

effectively not clearly discriminate scattering effects due to aerosols to absorption by CO₂ on the 1.6 μm band. However, we notice a scattering signature on the 2.06 μm band, quasi-independent of the CO₂ absorption. We can observe it on the Fig. 8-bottom, where the same Jacobians as top of figure are represented, but this time on the 2.06 μm band. We can reasonably assume that the fringe's contrast variations at the 6 mm OPD depends mainly of the scattering effects. This contrast variation is caused by the differential evolution of the edge of saturated lines of the 2.06 μm band affected by scattering, in contrast to the bottom. Thus a differential measurement of fringe contrast on 2.06 μm band at 6 mm and 12 mm (apparently not affected by scattering) allows to detect aerosol effects. This is a very promising mitigation way, with our limited number of samples over the interferogram. We are currently investigating the 760 nm band for mitigate the other potential geophysical biases. The next step will consist in studying the instrumental biases such as thermal variations.

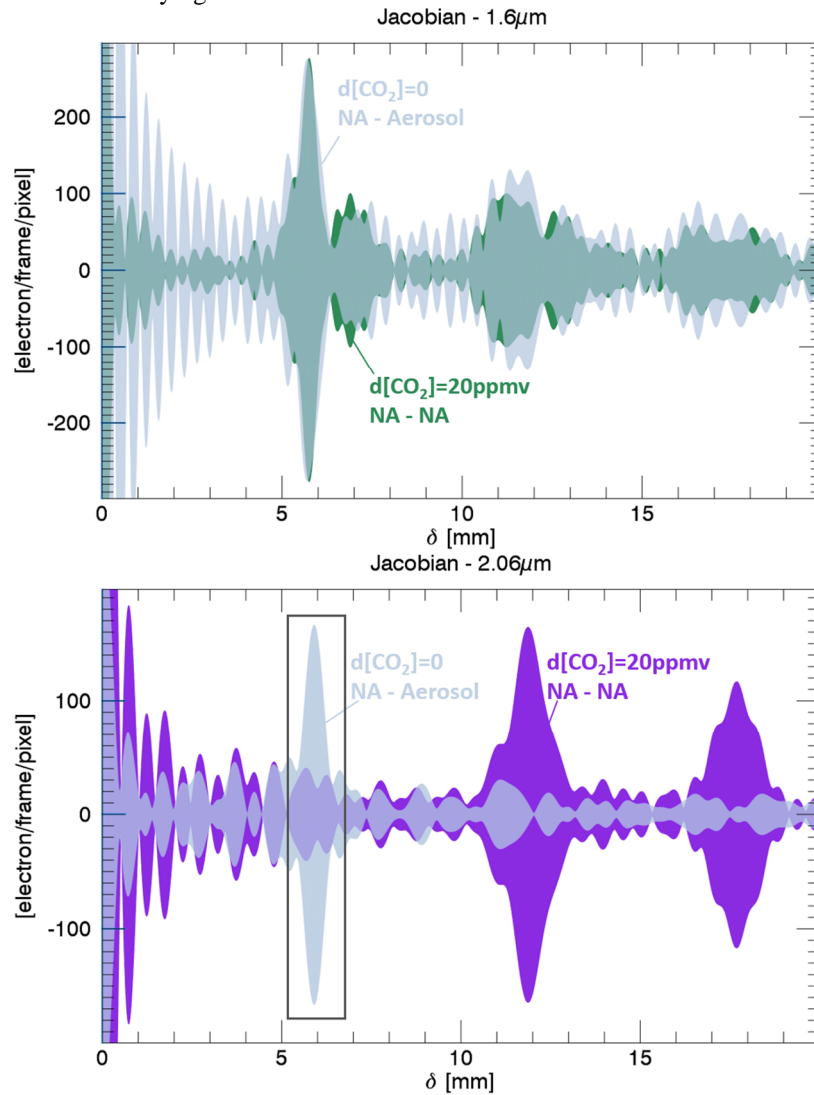


Fig. 8. Effects of scattering on the 1.6 μm (top) and 2.06 μm (bottom) bands. We notice a potential aerosol signature on the 2.06 μm band independent of CO₂ absorption. An interesting way to mitigated the relevant biases over the measure.

VI. CONCLUSION

We presented in this paper a very compact imaging-FTS for a 6U nanosatellite, dedicated to the temporal completion of data from the MicroCarb CNES mission. We propose an optimization of the instrument based on our numerical simulations of radiative transfer. We expect currently to compare precisely our simulations with more up-to-date CNES observational scenarios, in order to refine the design and expand the operational case number. The drastic miniaturization constraints of such an instrument are responsible for tradeoff about spectrum retrieval. Nevertheless, we demonstrated here that it is possible to extract some very specific information from the FTS data. Thus we reach a very high sensitivity better than 1 ppm of CO₂ in medium flux conditions, with only 100 samples over the interferogram. We have also the capability to detect scattering effects due to aerosols. We are currently studying on the same manner the mitigation of other kind of aerosol and geophysical biases such as water vapor. The next phase-0 studies will allow to analyze the instrumental biases induced over the measurement. We have also to determine SPOC calibration scenarios and navigation specifications.

As a conclusion the NanoCarb-21 mission has the capability to bring high temporally resolved data about CO₂ concentration to the MicroCarb mission. The SPOC technology is also promising for on-board compact spectrometry in science space-based applications. Indeed, we override the common weak points of the FTS, with a fully passive bulk instrument without mobile elements. Furthermore, this new kind of spectrometer allows to consider a break in terms of mass, volume and consumption power, and the possibility to make science with nanosatellites.

REFERENCES

- [1] T.F. Stocker, D. Qin, G.-K. Plattner, M. Tignor, S.K. Allen, J. Boshung, A. Nauels, Y. Xia, V. Bex and P.M. Midgley, "Contribution of Working Group I to the Fifth Assessment Report of the Intergovernmental Panel on Climate Change", in *Climate Change 2013: The Physical Science Basis*.
- [2] E.J. Dlugokencky, et al., "Global atmospheric methane: budget, changes and dangers", *Philos Trans A Math Phys Eng Sci*, 369, 2011.
- [3] P. Ciais, et al., "Current systematic carbon-cycle observations and the need for implementing a policy-relevant carbon observing system", *Biogeosciences*, 11, 3547-3602, 2014
- [4] E. le Coarer, B. Schmitt, N. Guerineau, G. Martin, S. Rommeluere, Y. Ferrec, F. Thomas, F. de la Barrière, T. Diard, "SWIFTS-LA: An Unprecedentedly Small Static Imaging FT Spectrometer" *Proceedings of the International Conference on Space Optics*, (2014).
- [5] P. Hébert, E. Cansot, C. Pierangelo, C. Buil, F. Brachet, F. Bernard, J. Loesel, T. Trémas, L. Perrin, E. Courau, C. Casteras, and I. Maussang, "From the Concept to the Definition of the SIFTI Instrument: Static Infrared Fourier Transform Interferometer", in *Advances in Imaging, OSA Technical Digest* (CD) (Optical Society of America, 2009)
- [6] E. Le Coarer, M. Barthelemy, A. Vialatte, M. Prugniaux, G. Bourdarot, T. Sequies, P. Monsinjon, R. Puget and N. Guerineau, "ATISE: a miniature Fourier transform spectro-imaging concept for surveying auroras and airglow monitoring from a 6/12U", *ICSO Biarritz, France*, 2016
- [7] A. Delannoy, B. Fièque, P. Chorier, C. Riuné, "NGP, a new large format infrared detector for observation, hyperspectral and spectroscopic space missions in VISIR, SWIR and MWIR wavebands". *Proc. SPIE 9639, Sensors, Systems, and Next-Generation Satellites XIX*, 96390R (October 12, 2015)
- [8] A. Berk, G. P. Anderson, P. K. Acharya, L. S. Bernstein, L. Muratov, J. Lee and R. B. Lockwood, "MODTRAN 5: a reformulated atmospheric band model with auxiliary species and practical multiple scattering options: update", In *Defense and Security* (pp. 662-667). International Society for Optics and Photonics. (2005, June).

